A CRITICAL DISTANCE APPROACH APPLIED TO MICROSCOPIC 316L BIOMEDICAL SPECIMENS UNDER FATIGUE LOADING

S.A. Wiersma and D. Taylor
Department of Mechanical and Manufacturing Engineering, Trinity College Dublin,
Dublin 2, Ireland
dtaylor@tcd.ie

Abstract

Fatigue tests were carried out on several types of 316L stainless steel specimens that were based on a biomedical microscopic component: the stent. Stents are used to scaffold open blocked arteries in people who suffer from the disease atherosclerosis. These small components are affected by fatigue because the arteries in which they are placed expand and contract with the beating of the heart. The Theory of Critical Distances (TCD) was used to predict the fatigue behaviour in the specimens containing notches similar to those found in stents. The TCD approach, which has been used previously on several macroscopic components containing long cracks, had to be altered to be able to describe the different fatigue behaviour in microscopic components containing short cracks. Crack closure is the most likely cause for the difference found. The altered method, based on the closure-free threshold value, gave good results for the tested specimen geometries.

Introduction

People who suffer from the disease atherosclerosis experience a severe reduction in artery diameter caused by the formation of a fatty deposit called plaque. As a result of this stenosis, less blood and therefore oxygen can flow downstream from the blockage, which can eventually lead to a heart attack. Stents were developed as a remedy against this disease, (Sigwart *et al* [1]). The stent is inserted in the vessel mounted on a catheter and a balloon and navigated to the position of the blockage. When the blockage is reached, the stent is expanded by expansion of the balloon. The material of the stent is hereby plastically deformed, thus trapping the plaque between the stent and the arterial wall and fixing it inside the artery. The balloon is then deflated and removed along with the catheter. The stent remains inside the artery as a permanent reinforcement, see Fig. 1.

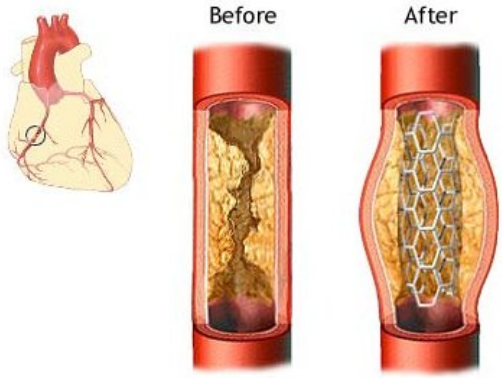

FIGURE 1. Atherosclerosis and the stent.

Because stents are placed inside the human body and subjected to fatigue loading, it is important to investigate the fatigue crack growth behaviour in these small components. Especially the bends and corners in the stent designs are susceptible to fatigue failure. The type of stent on which this work is based is laser cut from a piece of tubing. Typical sizes in these laser cut stent wires are around 0.1 mm.

Materials and Methods

Fatigue tests were carried out in tension on both macroscopic and microscopic 316L stainless steel specimens in order to investigate the influence of the specimen size on the fatigue crack growth behaviour. The focus of this work lies on the microscopic specimens, therefore, beside the plain macroscopic 316L stainless steel bar material, only one type of macro-scale circumferentially notched bar geometry was tested. This bar had an outer diameter of 12 mm and a notch depth of 1 mm.

Seven different microscopic stent-like notches were fatigue tested in tension: three types of double edge notched wire specimens, three types of slotted tubing pieces and one type of the original double edge notch wire geometry with a sharpened root radius on one notch. The thickness of all specimens was 90 microns. The net section width of all microscopic wire specimens was 110 microns and the net width of the slotted tubing pieces varied for the three different slot lengths. The tubing has an outer diameter of 1.7 mm. The micro-scale specimens were manufactured using the same process used to make stents: laser cutting, annealing and electro-polishing. Fig. 2 shows the micro-scale specimen geometries that were tested and the corresponding names that will be used.

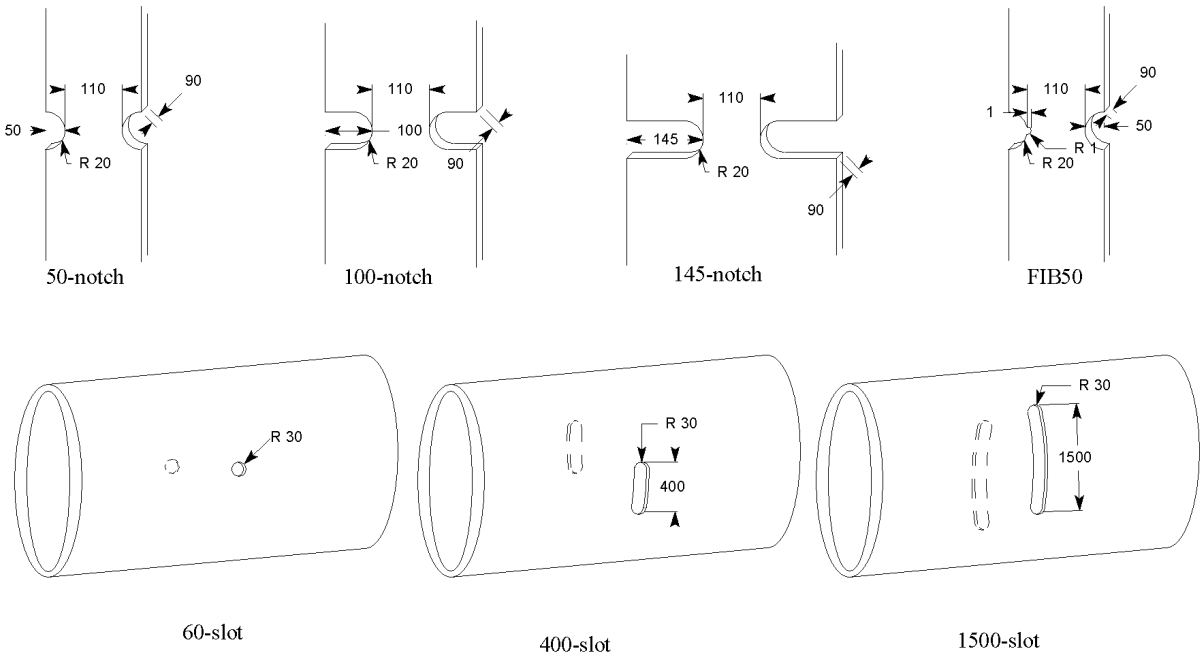

FIGURE 2. Geometry of the microscopic 316L stainless steel specimens.

The Theory of Critical Distances (TCD) was used to predict the fatigue behaviour of the microscopic specimens. This fracture mechanics based method was developed as a fatigue prediction method for macroscopic components, e.g. in the automotive and aerospace industry, (Taylor [2]). It determines the fatigue strength of a specimen or component by either analysing the stress at a certain critical point ahead of the stress concentration or averaging the stress over a certain critical distance ahead of the stress concentration and comparing it to the critical stress of the material: the plain specimen fatigue limit $\Delta\sigma_o$. These two variations are referred to as the Point Method (PM) and the Line Method (LM) and are similar to respectively Peterson's [3] and Neuber's [4] critical point and critical distance ideas. The problem with Peterson's and Neuber's equations is that at that the time Finite Element Analysis (FEA) was not as common as it is now, so approximations of the stress field ahead of the stress concentration had to be used, which only use the root radius of the geometry. The TCD, on the other hand, is capable of making predictions for specimens and components of arbitrary geometry using FEA to describe the elastic stress field ahead of the stress concentration.

The Point Method (PM) determines the stress at a critical point $L/2$ ahead of the stress concentration and the Line Method (LM) averages the stress over a distance of $2L$ ahead of the stress concentration. The parameter L is the critical distance of the material and is defined as follows:

$$L = \frac{1}{\pi}\left(\frac{\Delta K_{th}}{\Delta\sigma_o}\right)^2 \tag{1}$$

where ΔK_{th} is the long crack threshold stress intensity factor and $\Delta\sigma_o$ is the plain specimen fatigue limit, also based on long cracks in macroscopic specimens. Critical distance L is therefore a material property. The TCD method could not be used in its original form, because for the microscopic double edge notch wire specimens, the critical point for the PM ($L/2$) was positioned past half the width of the specimen, which made no sense and for the LM the critical distance $2L$ over which the stress is averaged, was larger than the specimen width and could therefore not be used, see Fig. 3.

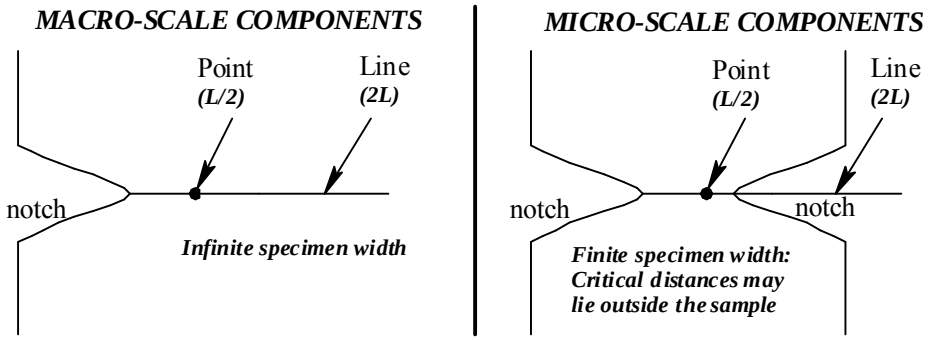

FIGURE 3. TCD cannot be used for micro-scale components if L is too large.

The original method uses the constant long crack material threshold value ΔK_{th} to determine the critical distance L. However, the threshold value reduces with crack length. In microscopic specimens a crack is always a short crack, even if it grows to failure. A short crack will never reach the constant long crack threshold value and therefore we hypothesized

that, for short cracks in microscopic specimens, the critical distance should be based on a reduced threshold value to reflect this difference.

This can be illustrated using the Resistance curve, which plots the stress intensity threshold vs. the crack length. Fig. 4 plots the R-curve for a fictitious material according to Tanaka and Nakai [5]. Tanaka assumes that even at low stress intensities a crack will grow until it is stopped by the first microstructural boundary, e.g. the grain boundary. The situation is shown for the maximum crack length in a micro-scale component, a_{micro}, where the corresponding threshold value is below the maximum constant value, similar to the situation for the microscopic specimens tested in this work.

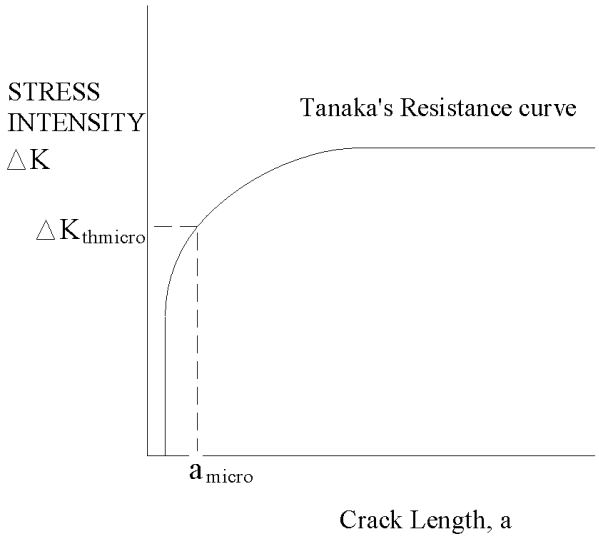

FIGURE 4. Tanaka's Resistance curve, showing how threshold changes with crack length.

The reason for this reduction in threshold value is most likely the lack of closure experienced by short cracks. Crack closure, (first discovered by Elber [6]), is a reduction in the effective stress intensity range, and therefore in the crack growth rate, due to the crack faces touching. For a short crack, the wake of the crack has not yet developed and therefore, no closure will occur. The effective, or closure-free, threshold value of the material can be determined through experimental testing at a high R-ratio (typically above 0.6). We used a new critical distance for micro-scale components or specimens, defined as L_{eff}:

$$L_{eff} = \frac{1}{\pi}\left(\frac{\Delta K_{effth}}{\Delta \sigma_o}\right)^2 \tag{2}$$

where ΔK_{effth} is the effective threshold of the material.

Results

Table 1 summarises the experimentally determined fatigue limit values for all the tested specimen geometries. All fatigue tests were carried out at an R-ratio of 0.1, apart from one series of circumferentially notched macro-scale bar specimens at an R-ratio of 0.8 to determine the effective closure-free threshold of the material.

The stress values quoted are calculated using the net section of the specimens. The fatigue data were generally found to level off at two million cycles, which is where the fatigue limits were determined. Non-failure points agreed with that choice, because they were also found around the fatigue limit.

TABLE 1. Summary of fatigue results.

MACRO	**Fatigue Limit at net section at 2 million cycles to failure [MPa]**						
	Plain bar		Notched bar		Notched bar (R=0.8)		
	420		150		75		
MICRO	**Fatigue Limit at net section at 2 million cycles to failure [MPa]**						
PLAIN	50-notch	100-notch	145-notch	FIB50	400-slot	60-slot	1500-slot
420	360	355	350	320	250	120	115

Table 2 summarizes the corresponding threshold values that were calculated for the tested notched macroscopic and microscopic specimens, assuming the notches to be sharp cracks in each case. The threshold was found to reduce for the microscopic specimens compared to the macroscopic threshold of 7.87 MPa√m. All microscopic specimen threshold values are similar and lie below the effective threshold value of 3.93 MPa√m.

TABLE 2. Summary of threshold results.

MACRO	**Threshold values [MPa√m]**						
	Notched bar				Notched bar (R=0.8)		
	7.87				3.93		
MICRO	**Threshold values [MPa√m]**						
	50-notch	100-notch	145-notch	FIB50	400-slot	60-slot	1500-slot
	2.73	2.89	2.91	2.43	2.38	2.59	3.07

Discussion

Fig. 5 shows the error values for predictions made using the original TCD method (using L) based on macroscopic material properties and the altered method, using the reduced effective threshold (L_{eff}). As expected, the original method gives large errors. The altered method is much better. Negative errors are non-conservative errors, which means that the method predicts the component or specimen to be stronger than it actually is.

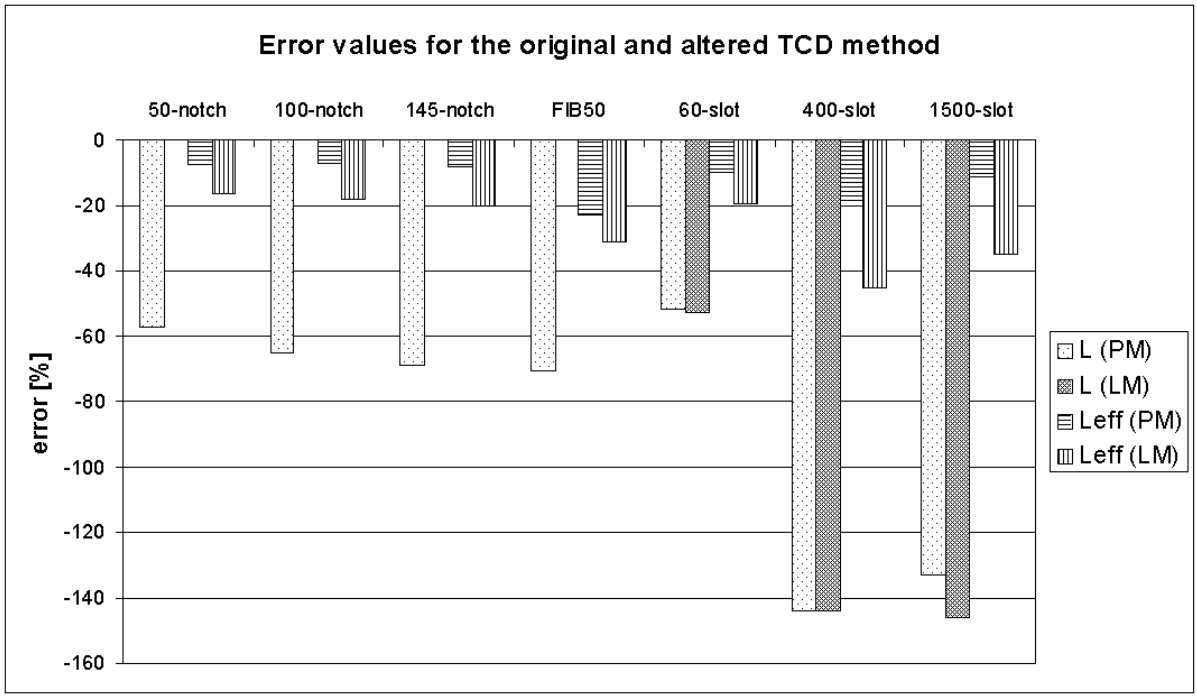

FIGURE 5. Prediction errors using the original TCD (using L) and the altered TCD (using L_{eff}).

Some error values were omitted in Fig. 5 for the original TCD Line Method. The reason is that the net section of these specimens was smaller than $2L$, making the prediction impossible. For the altered TCD method LM predictions could be made for the wire specimens, because the effective threshold reduced the value of L_{eff} to a length where $2L_{eff}$ is within the net section of the wire specimens.

Error values below 20% are considered acceptable, given the likelihood of 10% errors in the experimental data and the FEA. The altered PM gave excellent results, its worst prediction being of the FIB50 specimen, which is similar to the 50-notch, but with one sharpened notch. The idea behind this specimen was to consider if sharpening the notch would reduce the fatigue strength. Judging by the TCD predictions, this should not happen and in fact, this analysis was supported by the experimental results. The FIB50 fatigue limit differs by only 11% from that of the 50-notch specimen. The reason why the FIB50 PM error value is slightly above 20% is probably due to manufacturing problems that caused variations in the notch geometry, leading to more scatter. But, in general, the altered PM worked very well, not only for the wire specimens, but also for the tubing specimens. The difference between the wire and the tubing specimens is that the wire specimens are microscopic in both the thickness and the net width, while the tubing specimens are microscopic in the thickness, but have a macroscopic net section. The reduced critical distance was capable of predicting both types of specimen.

The altered Line Method gave good results for the wire specimens, but problems were encountered with the tubing specimens. The Line Method is more susceptible to the stress gradient of the stress concentration, because it averages the stress value over a certain distance instead of analysing the stress at just a point. In conclusion: the altered TCD Point Method gives excellent results for all microscopic specimens, the altered Line Method has problems with the tubing samples.

These altered methods were based on the expected difference between macro- and micro-specimens being due to the lack of crack closure, justifying the use of a closure-corrected value of L. We also considered two other possible reasons for the reduction in threshold and corresponding critical distance values in microscopic specimens: non-propagating cracks and plane stress/mode-III failure. The argument has been made that the critical distance might be related to the length of non-propagating cracks at the notch. An analysis using R-curves showed that the non-propagating crack length does reduce for microscopic specimens thus suggesting that the critical distance should also be reduced. However, this argument did not apply to some of the specimens, especially the 1500-slotted specimen, which contains a relatively long notch for which a full-length non-propagating crack was expected.

The very small thickness of the specimens suggested that a plane stress/mode-III failure might be occurring, which could also explain the reduced threshold. However this was shown not to be the cause, because in that case, the fracture surface should be at an angle of 45 degrees and not horizontal as was found for all microscopic specimens. Therefore, we conclude that the most likely cause is the lack of closure experienced by the microscopic specimens. This is why the effective threshold, in combination with the Point Method, was capable of predicting the data from all the microscopic specimens, including the 1500-slot. It seems that if the thickness is microscopic even relatively long cracks behave as short cracks.

Fig. 6 plots the threshold values for the microscopic wire and tubing specimens. The effective threshold value is given as a reference. The FIB50 sample is not included in the wire relation, because this geometry showed more scatter in the results because of the manufacturing difficulties. The graph illustrates that the threshold value is relatively constant but does tend to increase with increasing notch depth.

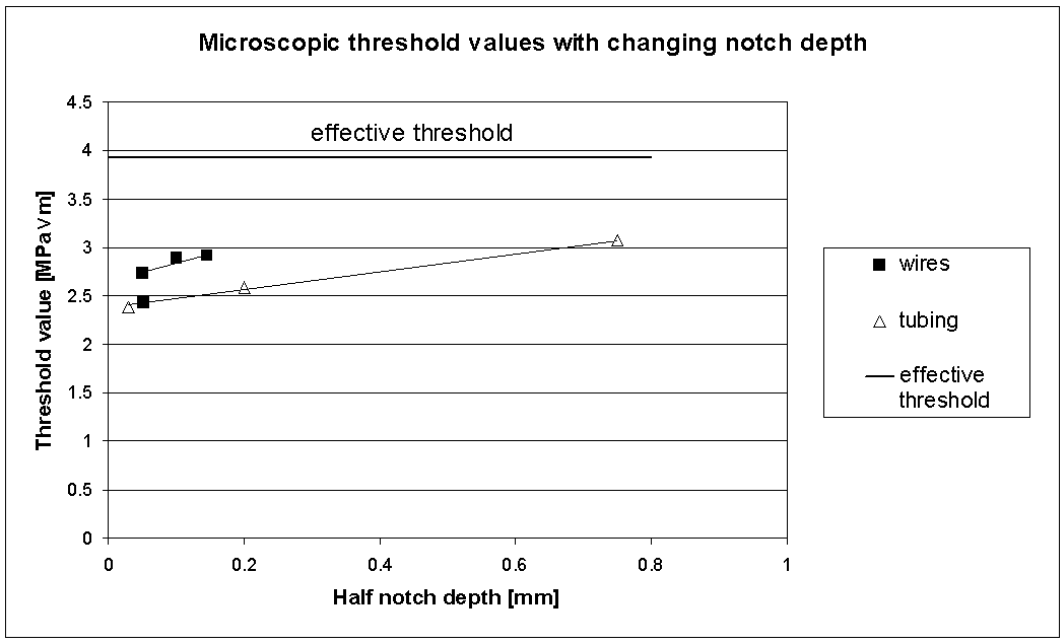

FIGURE 6. Threshold values against half notch depth for the microscopic specimens.

The threshold values of the microscopic specimens are lower than the effective threshold value. This difference – the extra reduction in threshold below the closure-free value – merits

further investigation: this may be due to the varying length of non-propagating cracks. We found even lower prediction errors if L was calculated using the average of these threshold values, though of course this approach implies the existence of data from at least one microscopic specimen.

Conclusions

1. The altered Point Method was capable of predicting all the tested microscopic 316L stainless steel fatigue data, after it had been altered to allow for the closure-free conditions of crack growth in these specimens.
2. Reduced threshold values were found for the microscopic specimens compared to the long crack macroscopic threshold value. Very good predictions could be made by using the average of these threshold values along with the PM.
3. Crack closure is likely to be the cause of the reduced thresholds found in the microscopic samples. However, maybe non-propagating cracks are the cause for the extra reduction in threshold found compared to the closure-free effective threshold value.
4. This method can easily be applied to other microscopic components, assuming that suitable material test data are available from which to calculate the necessary constants.

References

1. Sigwart, U., Puel, J., Mirkovitch, V., Joffre, F. and Kappenberger, L., *New England Journal of Medicine*, vol. **316**, 701-707, 1987.
2. Taylor, D., *International Journal of Fatigue*, vol. **21**, 413-420, 1999.
3. Peterson, R.E., In *Metal Fatigue*, edited by G. Sines and J.L. Waisman, McGraw Hill, New York, 1959, 293-306.
4. Neuber, H., *Theory of notch stresses*, Springer, Berlin, Germany, 1958.
5. Tanaka, K. and Nakai, Y., *Fatigue of Engineering Materials and Structures*, vol. **6**, 315-327, 1983.
6. Elber, W., *Engineering Fracture Mechanics*, vol. **2**, 37-45, 1970.